Journal of Pharmaceutical and Biomedical Analysis 137 (2017) 163–169

Contents lists available at ScienceDirect

Journal of Pharmaceutical and Biomedical Analysis

journal homepage: www.elsevier.com/locate/jpba

Impedimetric nanostructured genosensor for detection of schistosomiasis in cerebrospinal fluid and serum samples

Giselle S. Santos[a], Cesar A.S. Andrade[b], Igor S. Bruscky[c], Leandro B. Wanderley[d], Fabio L. Melo[e], Maria D.L. Oliveira[a,b,*]

[a] Programa de Pós-Graduação em Ciências Biológicas, Universidade Federal de Pernambuco, 50670-901 Recife, PE, Brazil
[b] Departamento de Bioquímica, Universidade Federal de Pernambuco, 50670-901 Recife, PE, Brazil
[c] School of Medicine, University of Pernambuco, Recife, Pernambuco, Brazil
[d] Aggeu Magalhaes Research Center/FIOCRUZ, Recife, Pernambuco, Brazil
[e] Laboratório de Doenças Transmissíveis, Centro de Pesquisas Aggeu Magalhães, 50670-420 Recife, PE, Brazil

ARTICLE INFO

Article history:
Received 26 November 2016
Received in revised form 12 January 2017
Accepted 14 January 2017
Available online 20 January 2017

Keywords:
Biosensors
Schistosomiasis
DNA
Cyclic voltammetry
Impedance spectroscopy
Metal nanoparticles

ABSTRACT

Schistosomiasis is a neglected disease closely related to the low levels of social development and a serious public health problem. In this work, we performed an electrochemical detection of *Schistosoma mansoni* DNA with a self-assembled monolayer of mercaptobenzoic acid (MBA) immobilizing nanostructures composed of gold nanoparticles (AuNPs) and magnetite nanoparticles (Fe_3O_4_NPs). Electrochemical impedance spectroscopy (EIS) and cyclic voltammetry (CV) were used to monitor the hybridization process. MBA-Fe_3O_4_NPs-AuNPs-DNAprobe system reveals an effective electrochemical response indicating the surface modification. The proposed biosystem was capable to recognize specific nucleotide sequence of *S. mansoni* present in cerebrospinal fluid (CFS) and serum samples at different genome DNA concentrations. The biorecognition resulted in an increase in the electron transfer resistance and a decrease of the current peaks at higher DNA concentrations during electrochemical measurements. The developed platform showed a DNA detection limit of 0.781 and 0.685 pg μL^{-1} for serum and CFS, respectively. Therefore, the obtained biosensor can be considered as a useful tool for specific detection of *S. mansoni* at low concentrations in various biological fluids.

© 2017 Elsevier B.V. All rights reserved.

1. Introduction

Schistosomiasis is an important parasitic disease for public health caused by helminth *Schistosoma mansoni* [1], which can be found in many tropical regions of the globe [2]. Some studies have reported six to seven million people affected in Brazil [3,4] with higher prevalence in Northeast states [2] and Southeast states [5,6].

A severe form of *S. mansoni* is the ectopic schistosomiasis that can manifest in different ways, especially involving the nervous system [7]. In these infections, spinal cord is more frequently affected than the brain [8]. The early treatment of the disease is essential for a good prognosis and preventing indiscriminate use of drugs by patients. Therefore, it is necessary the development of affordable diagnostic techniques with high sensibility and specificity [9]. Schistosomiasis diagnosis is based on the analysis of faecal samples and cerebrospinal fluid (CSF) for nervous system manifestation [7,10]. Some diagnostic tests such as ELISA, indirect fluorescence immunoassay, radioimmunoassay are also commonly used [11]. In general, diagnostic tests require expensive equipment and supplies, specialized technicians and are time-consuming [12].

The embolization of eggs during *S. mansoni* infection is the most important mechanism to reach the spinal cord. In addition, it is involved to endemic cases of neuroschistosomiasis in Brazil's Northwest [13]. Diagnostic methods for spinal cord schistosomiasis have low sensitivity and specificity. The definitive diagnosis of schistosomiasis is often a difficult process [14]. Therefore, an effective diagnosis is important, since early treatment can minimize sequelae [15,16].

Polymerase chain reaction (PCR) can be used to diagnose schistosomiasis in several biological samples [17], but its value in the CSF is still unknown. Some authors proposed the use of nested PCR to auxiliary the diagnosis of spinal cord schistosomiasis, in particular for cases with negative CSF serology [18]. However, further studies are needed to confirm its clinical use.

* Corresponding author at: Departamento de Bioquímica, UFPE, 50670-901 Recife, PE, Brazil.
E-mail address: m_danielly@yahoo.com.br (M.D.L. Oliveira).

http://dx.doi.org/10.1016/j.jpba.2017.01.031
0731-7085/© 2017 Elsevier B.V. All rights reserved.

In this context, electrochemical genosensors have been used as an excellent alternative for the development of new methods for diagnosis [19,20]. Electrochemical techniques reveal changes in the electrical properties of the electrode surface such as resistance and capacitance [21]. Impedimetric nanosensors are promising due to their potential for rapid detection of DNA sequences with low cost and sensitivity [21,22].

On the other hand, biosensors have appeared as an alternative to easy-to-handle, sensitive and low-cost diagnostic technology [23,24]. The advantages of the biosensors include the use of small amount of samples, reduced cost, portability, multiplexing capability and scalable for high-throughput applications. However, there are some issues to overcome such as stability, immobilization of biomaterials and interfacing of the systems between laboratories and clinics [25].

The association of metal nanoparticles have yielded nanostructured materials with distinctive properties [26]. Of note, the improved electroanalytical performance of nanostructured sensors is attributed to their high conductivity, large surface area, stability and biocompatibility [27]. In particular, optical, magnetic and catalytic properties of solid surfaces can be improved using magnetite (Fe_3O_4_NPs) and gold nanoparticles (AuNPs) [28–30]. Fe_3O_4_NPs and AuNPs have been used as platforms for the development of biosensors due to the ability to provide a stable immobilization of large amount of biomolecules and improvement of the biocompatibility [31,32].

In this work, we reported the construction of new highly sensitive electrochemical genosensor based on self-assembled monolayers of mercaptobenzoic acid (AMB) for *S. mansoni* detection. Aminated-Fe_3O_4_NPs and AuNPs were immobilized on AMB layers (Fig. 1). To the best of our knowledge this is the first time that an electrochemical platform is developed for specific detection of *S. mansoni*.

2. Experimental

2.1. Materials

S. mansoni samples were provided by the Parasitology Laboratory Aggeu Magalhães Research Center (Recife, Brazil). All samples were previously characterized using RT-qPCR. Mercaptobenzoic acid (AMB), gold(III) chloride hydrate ($HAuCl_4 \bullet xH_2O$), (3-aminopropyl)triethoxysilane (APTES), trisodium citrate, bovine serum albumin (BSA), 1-[3-(dimethylamino)propyl]-3-ethylcarbodiimide hydrochloride (EDC) and N-hydroxysuccinimide (NHS) were purchased from Sigma-Aldrich (St. Louis, MO, USA). Ammonium hydroxide (NH_4OH), potassium ferri- and ferrocyanide were obtained from VETEC (Brazil). All other chemicals used in this work were reagent-grade quality and used as received without further purification. Ultrapure water was obtained from a Millipore Milli-Q system.

2.2. Sample preparation

CSF samples (1 mL) were obtained by lumbar puncture. CSF analyses were based on cell count, dosage of glucose and protein. In addition, protein electrophoresis and immunological determinations for others infections were evaluated [10].

Schistosoma DNA and genomic material from cerebrospinal serum fluid were purified using the illustra tissue and blood genomic Prep Mini Spin Kit (GE Healthcare, UK) in according to the manufacturer's instructions. The thiolated primer was specific for *S. mansoni* with the sequence Schfo17 (5′-GTGCTGGT GGGTTGACGAGTTC-3′) [33].

2.3. Synthesis of nanoparticles

Gold nanoparticles were synthesized in according to Frens [34]. A mixture of $HAuCl_4$ and trisodium citrate was obtained. 100 mL of the first solution (0.01 wt% $HAuCl_4 \cdot H_2O$) was boiled under vigorous stirring in a flask. Furthermore, 2.5 mL of trisodium citrate solution (1% w/v) was added quickly to the boiling solution, resulting in a color change from yellow to red, indicating the formation of AuNPs. Then, the solution was maintained at boiling temperature for 10 min.

APTES-modified Fe_3O_4_NPs were obtained according to Gan et al. [35]. Initially, 0.2 g Fe_3O_4_NPs were added to 90 mL ethanol. Subsequently, 2 mL NH_4OH (25%) and 300 μL APTES were added to the previous solution, and stirred overnight. Then, the product was magnetically separated and washed three times with deionized water to obtain aminated-Fe_3O_4_NPs.

2.4. Electrode modification

The bare gold electrode (BGE) was polished with sandpaper and deionized water. Subsequently, BGE was immersed in a piranha solution for 5 min, dried at room temperature and incubated with 2 μL AMB after washing with deionized water. Then, 2 μL of equal parts (1:1) of 0.4 M EDC and 0.1 M NHS was added on the electrode surface for a period of 10 min in order to activate AMB carboxylic groups. After this, 2 μL aminated-Fe_3O_4_NPs was dropped on the MBA-EDC/NHS-modified electrode following incubation for 10 min. Then, the residual protonated amine groups of MBA-Fe_3O_4_NPs was modified with AuNPs to obtain (MBA-Fe_3O_4_NPs-AuNPs) using the same EDC/NHS method. Finally, thiolated DNA probe was immobilized on the AuNPs surface. Fig. 1 shows the manufacturing process of the MBA-Fe_3O_4_NPs-AuNPs-DNAprobe system. BSA was used in all experiments to avoid non-specific interactions.

2.5. Hybridization analysis

Target DNA was diluted in 10 mM phosphate-buffered saline (PBS) solution (pH 7.4) and heated (3 min at 40° C) before the experiments. The hybridization was carried out by simple drop-coating technique using 2 μL of the target DNA obtained from biological samples at different concentrations.

2.6. Electrochemical measurements

Electrochemical analyses were performed using a PGSTAT 128N potentiostat/galvanostat (Autolab, Netherlands) with a three electrode conventional electrochemical cell interfaced with an analyzer controlled by a computer. All experiments were performed in the presence of a 10 mM $K_4[Fe(CN)_6]^{4-}/K_3[Fe(CN)_6]^{3-}$ solution (1:1) used as a redox probe. BGE was used as work electrode. Platinum wire electrode and Ag/AgCl (saturated KCl) were used as auxiliary and reference electrodes, respectively. Impedimetric assays were performed at a frequency between 100 mHz and 100 kHz, with amplitude of the applied sine wave potential of 10 mV. CV analyses were obtained in the range of potentials between +0.7 V and −0.2 V at a scan rate of 50 mV s^{-1}. All electrochemical measurements were performed in triplicate using three different samples (n = 3).

2.7. Atomic force microscopy measurements

Topographic analysis of the system were performed through an atomic force microscope (SPM-9700, Shimadzu Corporation, Japan) in a noncontact mode in air at room temperature (approximately 25 °C) [36]. Cantilevers with a silicon AFM probe (Nanoworld, Japan, resonant frequency = 300 kHz, spring constant = 42 N m^{-1})

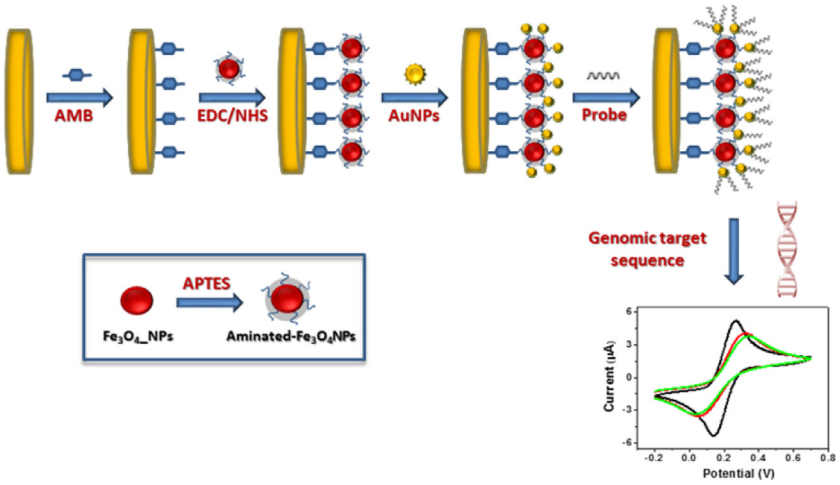

Fig. 1. Schematic representation of the surface modification.

were used. The images (512 points per line) were collected with a scan rate of 1.0 Hz in a scan area of 7.0 × 7.0 μm. In addition, images were obtained and analyzed using AFM Gwyddion software [37].

3. Results and discussion

3.1. Topographic evaluation

Fig. 2a shows MBA modified-BGE surface with the presence of peaks distributed along of the BGE surface and roughness about 56 nm. Then, after modification of MBA self-assembled layer with Fe_3O_4_NPs and AuNPs, it can be observed the presence of small-dispersed nanoparticles with a heterogeneous distribution on the surface (Fig. 2b). Subsequently, DNA probe immobilization results in a surface roughness of 84 nm (Fig. 2c), in accordance to previous results reported in the literature [29,38]. The interaction between *S. mansoni* sample and the sensor surface was evaluated and significant changes in the topography were observed (Fig. 2d). However, the binding of a non-complementary target does not cause significant changes (Fig. 2e), demonstrating the specificity of the sensor.

3.2. Voltammetric characterization

Fig. 3a shows the voltammetric response of the stepwise fabrication process of the sensor. Initially, BGE voltammetric curve showed a characteristic behavior of a process limited by diffusion of the redox probe. As explained before, BGE was subsequently modified with MBA, which contains a thiol group enabling its adsorption on the metal surface and resulting in a self-assembled monolayer [39–42]. In addition, MBA contains a carboxylic acid functional group that allows a covalent bond with modified nanoparticles [43]. A decrease of the anodic and cathodic peaks is observed due to MBA adsorption. After, MBA carboxylic acid moiety was activated using EDC/NHS coupling reagents. During the reaction, NHS ester group replaced the carboxyl group of AMB and, thus, provides an increase in the current response due to electrostatic interactions [44]. After immobilization of the aminated-Fe_3O_4_NPs on MBA-modified electrode, an additional decrease in the amperometric electrode response was observed. Subsequently, AuNPs is covalently binding to Fe_3O_4_NPs through EDC/NHS (Fig. 3a).

Finally, thiol-modified DNA probe was adsorbed on the MBA-Fe_3O_4_NPs-AuNPs to obtain the biosensor. MBA-Fe_3O_4_NPs-AuNPs-DNAprobe system revealed a decrease in the amperometric response of the electrode with semi-reversible behavior, since electron-transfer kinetics of $K_4[Fe(CN)_6]^{4-}/K_3[Fe(CN)_6]^{3-}$ is perturbed by hindrance of the electron diffusion (Fig. 3a). Therefore, after oligonucleotide immobilization a decrease of the redox probe penetration is observed. In particular, after hybridization process with complementary genome a decrease in the anodic and cathodic peaks was obtained (Fig. 3b) due to the specific interaction. Of note, the hybridization process on the electrode acts as a mass-transfer blocking layer and hinders the diffusion of ferricyanide toward the electrode surface [36,45].

3.3. Electrochemical impedance spectroscopy characterization

EIS technique provides a complete and detailed view of the electrical characteristics of the electrode/solution interface [36,46]. Fig. 4a shows the Nyquist plots of the stepwise electrode surface modification. A typical Cole–Cole semicircle with two well-defined regions containing a higher frequency region characterized by the electron transfer process and a lower frequency region limited by the diffusion process was obtained [47]. The BGE shows a very small semicircle domain (Fig. 4a) implying a very low electron-transfer resistance (Ret) of the redox probe. After, Ret was increased again after electrode modification using negatively charged MBA (Fig. 4a). Then, MBA acts as an electrostatic barrier that hinders the ability of the redox probe to access the electrode. EDC/NHS activation and subsequent immobilization of Fe_3O_4_NPs and AuNPs provide an additional Ret increase (Fig. 4). The nanoparticles were immobilized by a simple drop-coating procedure. A new increase in the Ret was obtained after association between DNA probe and MBA-Fe_3O_4_NPs-AuNPs-modified gold electrode (Fig. 4), indicating an obstruction of the electron transfer.

The impedance data were fitted to a modified Randles equivalent circuit (inset, Fig. 4a), which includes the solution resistance (Rsol), electron transfer resistance (Ret), constant phase element (CPE) and Warburg impedance element (W). Ideally, W and Rsol represent the bulk properties of the electrolyte solution and diffusion features of the redox probe in solution, respectively. In addition, W and Rsol components were not significantly affected by modifications of the electrode surface. CPE value is related to the ionic charges, surface area, dielectric constant and thickness of the layer [48]. Ret element depends on the insulating feature at the electrode/electrolyte interface. In the present study, the changes in Ret were more pronounced than those in other impedance components. Thus, Ret was used for sensing the interfacial properties of the developed genosensor for all assembly procedures.

The hybridization process was confirmed after successive blockage of the electron transfer at the sensor surface after

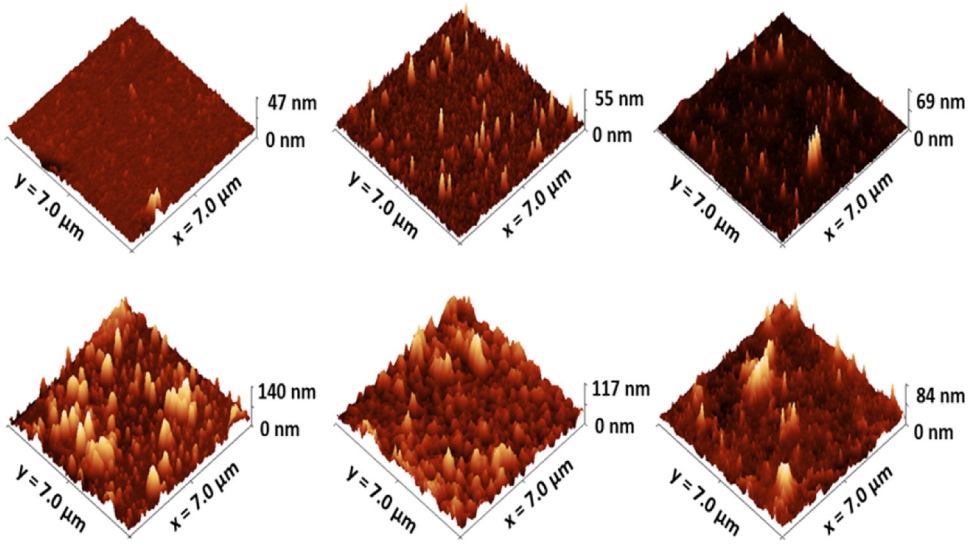

Fig. 2. AFM images of the stepwise modification process: a) MBA b) MBA-Fe_3O_4_NPs-AuNPs; c) MBA-Fe_3O_4_NPs-AuNPs-DNAprobe; d) MBA-Fe_3O_4_NPs-AuNPs-DNAprobe-DNA target; e) MBA-Fe_3O_4_NPs-AuNPs-DNAprobe-CSFgenome and, f) MBA-Fe_3O_4_NPs-AuNPs-DNAprobe-negative control.

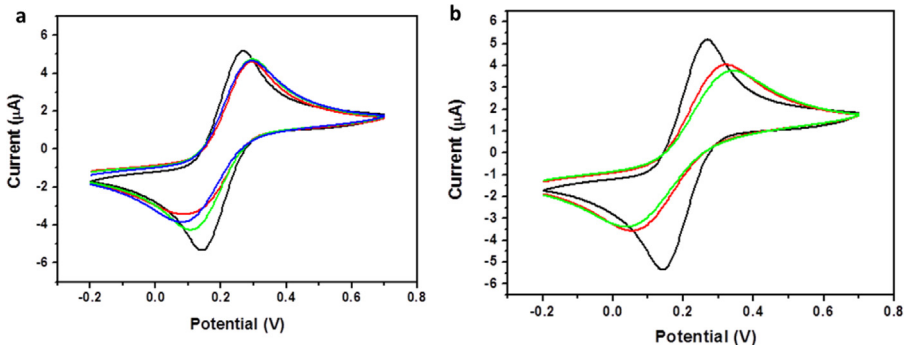

Fig. 3. Cyclic voltammograms of the stepwise modification process (a) and CVs at different stages of biorecognition process (b): BGE (—), MBA-Fe_3O_4_NPs-AuNPs-DNAprobe (▬), MBA-Fe_3O_4_NPs-AuNPs-probe-genome (▬). Cyclic voltammetry scan was initiated at − 0.2 V vs. Ag/AgCl in positive direction at 50 mV s^{-1}.

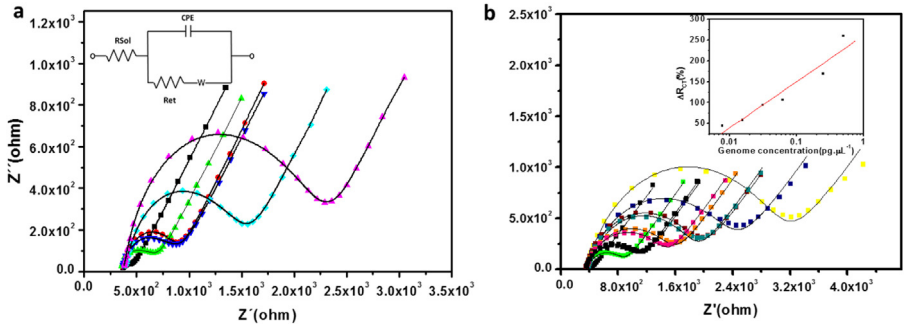

Fig. 4. (a) Nyquist plots of the stepwise modification and immobilization process: (■) BGE, (●) MBA, (▲) MBA-EDC/NHS, (▼) MBA-Fe_3O_4_NPs-AuNPs, (◆) MBA-Fe_3O_4_NPs-AuNPs-DNAprobe and (◀) MBA-Fe_3O_4_NPs-AuNPs-DNAprobe-genome. Inset: Equivalent circuit. (b) Biosensor response when exposed to different concentrations of target genomic DNA and a negative control: (■) BGE, (■) MBA-Fe_3O_4_NPs-AuNPs, (■) MBA-Fe_3O_4_NPs-AuNPs-DNAprobe, (■) Biosensor-genome (7.8 pg μL^{-1}), (■) Biosensor-genome (15.6 pg μL^{-1}), (■) Biosensor-genome (31.3 pg mL^{-1}), (■) Biosensor-genome (0.62 ng μL^{-1}), (■) Biosensor-genome (0.25 ng μL^{-1}), (■) Biosensor-genome (0.5 ng μL^{-1}), and (■) Biosensor-negative control. Inset: ΔRet% as a function of different concentrations of genomic target sequence. Solid lines represent the simulation results.

genome recognition. Five different concentrations of complementary *S. mansoni* genome (0.5 ng μL^{-1}, 0.25 ng μL^{-1}, 0.62 ng μL^{-1}, 31.3 pg μL^{-1}, 15.6 pg μL^{-1} and 7.8 pg μL^{-1}) were tested (Fig. 4b). A successive increase in the Cole–Cole semicircle is clearly visualized and proportional to the increment of DNA concentration, suggesting a specific interaction between the sensor and *S. mansoni* genome.

Table 1 shows the equivalent circuit parameters of the fitting curves for all measurements. The obtained results were consistent with CV curves shown in Fig. 3 and revealed a different response for each DNA concentration (Fig. 4). After hybridization process, we observed that the Ret values increased significantly, while a reduction of CPE values occurred at the same time. Of note, EIS spectra showed higher Ret values for positive samples than for negative

Table 1
Values of the equivalent circuit elements from fitted impedance results.

Modified electrode	[Genomic target sequence]	R_{CT}/kΩ	Q/μF	n
Bare gold electrode	–	0.15	1.63	0.36
MBA-Fe_3O_4_NPs-AuNPs_DNA probe	–	0.75	7.47	0.72
Serum Sample				
Genosensor	7.8 pg μL^{-1}	1.08	6.92	0.73
Genosensor	15.6 pg μL^{-1}	1.19	6.78	0.73
Genosensor	31.3 pg μL^{-1}	1.46	4.52	0.78
Genosensor	0.62 ng μL^{-1}	1.55	5.85	0.77
Genosensor	0.25 ng μL^{-1}	2.02	5.53	0.75
Genosensor	0.5 ng μL^{-1}	2.70	3.98	0.79
CSF Sample				
Genosensor	0.5 pg μL^{-1}	2.09	3.59	0.77
Genosensor	5.0 pg μL^{-1}	2.22	3.87	0.76
Genosensor	50 pg μL^{-1}	2.27	3.63	0.78
Genosensor	0.5 ng μL^{-1}	2.43	2.98	0.82
Sensor_DNA control negative	–	0.72	8.51	0.71

Table 2
Relative charge transfer variation from impedance data.

Condition	Before*	After[1]	After[2]	After[3]
		Serum Sample	CSF Sample	
Ret/KΩ	0.75	2.70	2.43	0.71
ΔRet (%)	–	260.0	224.0	30.6

Sensor response before interaction with genomic target sequence; 1 – after recognition of complementary genomic target sequence; 2 – after recognition of genomic target specific from CSF and, 3 – after contact with non-complementary genomic target sequence.

target indicating specific interactions between evaluated probe and genomic target.

The results presented in Fig. 4 clearly show that DNA probe was capable to recognize specific genomic target after immobilization as can be seen by the increase of the Ret. The performance of the modified electrode for detection of *S. mansoni* genome was evaluated through the relative variation of Ret (ΔRet). This variation can be calculated according to the following equation: $\Delta Ret(\%) = [(Ret_{PG} - Ret_P)/Ret_P] \times 100$, where Ret_P is the value of the electron-transfer resistance of the MBA-Fe_3O_4_NPs-AuNPs-DNAprobe-modified electrode. Ret_{PG} is the value of the electron-transfer resistance of the MBA-Fe_3O_4_NPs-AuNPs-DNAprobe-genome-modified electrode after exposing it to contaminated samples.

An impedimetric evaluation was performed for different concentrations of *S. mansoni* genome (Fig. 4b). A linear relationship between ΔRet and genome concentration was found and the detection limit was estimated to be approximately 0.78 pg.μL^{-1} (inset, Fig. 4b). ΔRet increases proportionally to *S. mansoni* genome concentration and indicates that the modified electrode can sense the interactions between the probe and genomic target.

In addition, the selectivity of the biosensor was evaluated by changes in the Ret response by incubating with complementary and non-complementary genomic sequences. We used non-complementary genomic sequence from Leishmaniasis as a negative control (0.1 ng μL^{-1}). The interaction of the biosensor with a negative control (non-complementary sequence) resulted in low values of Ret, revealing the selectivity of the bioelectrode. Two important widespread neglected tropical diseases are schistosomiasis and leishmaniasis. Of note, both parasitic diseases are associated to high impact in human health in endemic areas and double infection is not uncommon [49]. In addition, Schistosoma and Leishmania are important human parasites that share diverse clinical manifestations. The diagnosis can be difficult for either of infections and therefore it is important to distinguish between them [50].

A brief information of these results is given in Table 2, for fixed concentrations of genomic target sequence. These results demonstrate that the biosystem retains its capability to recognize specific target as a clear indication that this system could be used for specific detection of *S. mansoni* in clinical samples.

3.4. *Detection of* S. mansoni *in cerebrospinal fluid*

As previously explained, we developed a sensor platform capable of recognizing *S. mansoni* genome in different biological samples. Therefore, the biosensor was exposed to cerebrospinal fluid (CSF) to evaluate its effectiveness to other samples. The sensitivity could be observed by the increase of the Cole–Cole semicircle (Fig. 5a) with linear relationship between ΔRet and DNA concentration as shown in Fig. 5a (Inset). After electrochemical analysis we obtained a correlation coefficient of 0.96. This result indicates that the interactions between probe and genomic target sequence can be sensed by MBA-Fe_3O_4_NPs-AuNPs-DNAprobe system. The detection limit of 0.685 pg μL^{-1} was estimated from the relation of signal and noise characteristics of these data (S/N = 3). Significant increase in the Ret values were observed after recognition of positive samples (Table 1). Our detection limits were superior to previous reports using monoclonal antibodies for specific detection of *S. mansoni* [51,52]. Sensitivity was evaluated through a calibration curve obtained from impedimetric responses after exposure the genosensor to the target sample. Thus, the sensor platform showed good sensitivity being able to detect genomic target at low concentrations of genetic material in CSF.

The filling of the recognition sites (θ) can be calculated by $\theta = (1 - R_{system})/R_{hybridization}$, where R_{System} is the Ret of the biosensor and $R_{Hybridization}$ is the Ret of the biosensor after exposure to different concentrations of the genomic target sequence. Fig. 5b shows a plot of θ as a function of concentration of the genomic target sequence. The value of θ increases with increasing DNA target concentration and is found to be 0.69 (69%) at 5.0 ng μL^{-1}.

The reproducibility of the genosensor using at least three sensors fabricated independently at the same conditions was

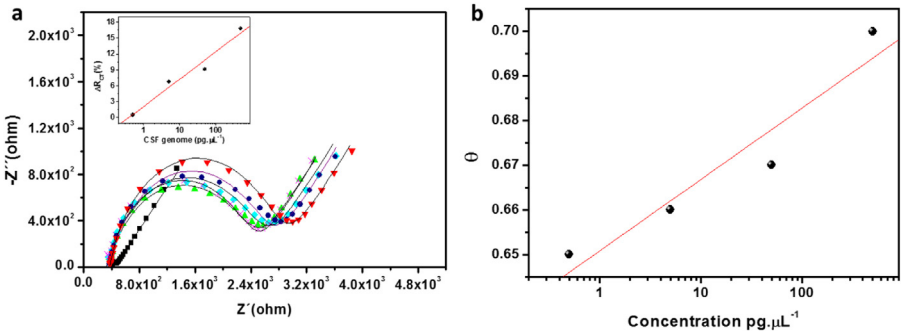

Fig. 5. (a) Nyquist plots of the biosensor when exposed to different concentrations of DNA genome obtained from CSF: (■) BGE, (▲) MBA-Fe_3O_4_NPs-AuNPs-DNAprobe, (◆) Biosensor-genome (0.5 pg μL^{-1}), (×) Biosensor-genome (5.0 pg μL^{-1}), (●) Biosensor-genome (50.0 pg μL^{-1}), (▼) Biosensor-genome (0.5 ng μL^{-1}). Inset: ΔRet%, and θ (b) as function of different concentrations of *S. mansoni* genome obtained from CSF.

evaluated and revealed a relative standard deviation (R.S.D.) of 4.2%. The proposed biosensor demonstrated simplicity, selectivity and sensitivity with 0.685 pg μL^{-1} LOD. In general, biosensors for schistosomiasis diagnosis are based on antibody-antigen recognition with LOD varying between 1.3 and 360 ng mL^{-1} [53,54] The proposed biosensor is effective with low volume of samples (2 μL) and assay time of 25 min. Therefore, MBA-Fe_3O_4_NPs-AuNPs-DNAprobe system is a useful platform for the development of biosensors for specific detection of *S. mansoni* in different biological fluids such as CSF and serum based on hybridization process.

4. Conclusion

Impedimetric and voltammetric analysis were used for the development of a specific biosensor for *S. mansoni*. The developed biosensor showed a good performance for determination of genomic target sequence from *S. mansoni* with low limit of detection, specificity and reproducibility. The developed sensor platform was effective in detecting *S. mansoni* in different biological fluids. These results confirmed that this sensing approach provides a rapid, sensitive and convenient way for detection of *S. mansoni*.

Acknowledgments

G.S. Santos would like to thank FACEPE for a MSc scholarship. M.D.L. Oliveira and C.S.A. Andrade would like to thank CNPq (grant 302885/2015-3 and 302930/2015-9) and INCT_if.

References

[1] S. Tomczyk, K. Deribe, S.J. Brooker, H. Clark, K. Rafique, S. Knopp, J. Utzinger, G. Davey, Association between footwear use and neglected tropical diseases: a systematic review and meta-analysis, PLoS Negl. Trop. Dis. 8 (2014) e3285.
[2] R.G. Scholte, L. Gosoniu, J.B. Malone, F. Chammartin, J. Utzinger, P. Vounatsou, Predictive risk mapping of schistosomiasis in Brazil using Bayesian geostatistical models, Acta Trop. 132 (2014) 57–63.
[3] T.C. Favre, A.P. Pereira, L.C. Beck, A.F. Galvao, O.S. Pieri, School-based and community-based actions for scaling-up diagnosis and treatment of schistosomiasis toward its elimination in an endemic area of Brazil, Acta Trop. 149 (2015) 155–162.
[4] C.H. King, Parasites and poverty: the case of schistosomiasis, Acta Trop. 113 (2010) 95–104.
[5] W. Tavares, L.A.C. Marinho, Rotinas De Diagnóstico E tratamento Das Doenças Infecciosas E Parasitárias, 2nd ed., Atheneu, São Paulo, 2007.
[6] D.S. Martins, M.F. Xavier, F.S. Masiero, J. Cordeiro, P.J. Thyssen, Schistosomiasis in Southern Brazil 17 years after the confirmation of the first autochthonous case, Rev. Soc. Bras. Med. Trop. 48 (2015) 354–357.
[7] T.C. Ferrari, P.R. Moreira, A.S. Cunha, Clinical characterization of neuroschistosomiasis due to Schistosoma mansoni and its treatment, Acta Trop. 108 (2008) 89–97.
[8] T.C. Ferrari, P.R. Moreira, Neuroschistosomiasis: clinical symptoms and pathogenesis, Lancet Neurol. 10 (2011) 853–864.
[9] G. Harter, H. Frickmann, S. Zenk, D. Wichmann, B. Ammann, P. Kern, B. Fleischer, E. Tannich, S. Poppert, Diagnosis of neuroschistosomiasis by antibody specificity index and semi-quantitative real-time PCR from cerebrospinal fluid and serum, J. Med. Microbiol. 63 (2014) 309–312.
[10] I.S. Bruscky, F.L. de Melo, Z.M. de Medeiros, F.F. Albuquerque, L.B. Wanderley, C. da Cunha-Correia, Nested polymerase chain reaction in cerebrospinal fluid for diagnosing spinal cord schistosomiasis: a promising method, J. Neurol. Sci. 366 (2016) 87–90.
[11] J.T. Coulibaly, N.K. N'Goran, J. Utzinger, M.J. Doenhoff, E.M. Dawson, A new rapid diagnostic test for detection of anti-Schistosoma mansoni and anti-Schistosoma haematobium antibodies, Parasites Vectors 6 (2013) 29.
[12] J. Clerinx, E. Bottieau, D. Wichmann, E. Tannich, M. Van Esbroeck, Acute schistosomiasis in a cluster of travelers from Rwanda: diagnostic contribution of schistosome DNA detection in serum compared to parasitology and serology, J. Travel Med. 18 (2011) 367–372.
[13] F.J. Carod-Artal, Neurological complications of Schistosoma infection, Trans. R. Soc. Trop. Med. Hyg. 102 (2008) 107–116.
[14] S.d.V.e.S. Ministério da Saúde, Guia de vigilância epidemiológica e controle da mielorradiculopatia esquistossomótica, Série A. Normas e Manuais Técnicos, Ministério da Saúde, Brasília, (2006) 1–32.
[15] B. Gryseels, Infect. Schistosomiasis, Dis. Clin. N. Am. 26 (2012) 383–897.
[16] A.G. Ross, P.B. Bartley, A.C. Sleigh, G.R. Olds, Y.S. Li, G.M. Williams, Schistosomiasis, N. Engl. J. Med. 346 (2002) 1212–1220.
[17] N. Sandoval, M. Siles-Lucas, J.L. Pérez-Arellano, C. Carranza, S. Puente, J. López-Aban, A. Muro, A new PCR-based approach for the specific amplification of DNA from different Schistosoma species applicable to human urine samples, Parasitology 133 (2006) 581–587.
[18] I.S. Bruscky, F.L. de Melo, Z.M. de Medeiros, F.F. Albuquerque, L.B. Wanderley, C. Cunha-Correia, Nested polymerase chain reaction in cerebrospinal fluid for diagnosing spinal cord schistosomiasis: a promising method, J. Neurol. Sci. 366 (2016) 87–90.
[19] P. Kara, C. Cavusoglu, S. Cavdar, M. Ozsoz, Direct electrochemical genosensing for multiple point mutation detection of Mycobacterium tuberculosis during the development of rifampin resistance, Biosens. Bioelectron. 24 (2009) 1796–1800.
[20] A.C.H. Castro, E.G. Franc, L.F. de Paula, M.M.C.N. Soares, L.R. Goulart, J.M. Madurro, A.G. Brito-Madurrosince, Preparation of genosensor for detection of specific DNA sequence of the hepatitis B virus is possible convert the hybridization into a measurable electric signal, Appl. Surf. Sci. 314 (2014) 273–279.
[21] A. Bonanni, M. del Valle, Use of nanomaterials for impedimetric DNA sensors: a review, Anal. Chim. Acta 678 (2010) 7–17.
[22] A. Guiseppi-Elie, L. Lingerfelt, Impedimetric detection of DNA hybridization: towards near-patient DNA diagnostics, Top. Curr. Chem. 260 (2005) 161–186.
[23] A.M. Foudeh, D.T. Fatanat, T. Veres, M. Tabrizian, Microfluidic designs and techniques using lab-on-a-chip devices for pathogen detection for point-of-care diagnostics, Lab. Chip. 18 (2012) 3249–3266.
[24] P. D'Orazio, Biosensors in clinical chemistry, Clin. Chim. Acta 19–20 (2011) 1749–1761.
[25] M.L. Sin, K.E. Mach, P.K. Wong, J.C. Liao, Advances and challenges in biosensor-based diagnosis of infectious diseases, Expert Rev. Mol. Diagn. 14 (2014) 225–244.
[26] C. Xu, J. Xie, D. Ho, C. Wang, N. Kohler, E.G. Walsh, J.R. Morgan, Y.E. Chin, S. Sun, Au-Fe3O4 dumbbell nanoparticles as dual-functional probes, Angew. Chem. Int. Ed. Engl. 47 (2008) 173–176.
[27] F. Li, X. Han, S. Liu, Development of an electrochemical DNA biosensor with a high sensitivity of fM by dendritic gold nanostructure modified electrode, Biosens. Bioelectron 26 (2011) 2619–2625.
[28] W. Wu, Q. He, C. Jiang, Magnetic iron oxide nanoparticles: synthesis and surface functionalization strategies, Nanoscale Res. Lett. 3 (2008) 397–415.
[29] R. Das, M.K. Sharma, V.K. Rao, B.K. Bhattacharya, I. Garg, V. Venkatesh, S. Upadhyay, An electrochemical genosensor for Salmonella typhi on gold nanoparticles-mercaptosilane modified screen printed electrode, J. Biotechnol. 188 (2014) 9–16.

[30] T. Rolim, J. Cancino, V. Zucolotto, A nanostructured genosensor for the early diagnosis of systemic arterial hypertension, Biomed. Microdevices 17 (2015) 3.
[31] S. Liu, J. Liu, L. Wang, F. Zhao, Development of electrochemical DNA biosensor based on gold nanoparticle modified electrode by electroless deposition, Bioelectrochemistry 79 (2010) 37–42.
[32] R.D. Zysler, E. Lima Jr., M.V. Mansilla, H.E. Troiani, M.L.M. Pisciotti, P. Gurman, A. Lamagna, L. Colombo, A new quantitative method to determine the uptake of SPIONs in animal tissue and its application to determine the quantity of nanoparticles in the liver and lung of balb-c mice exposed to the SPIONs, J. Biomed. Nanotechnol. 9 (2013) 142–145.
[33] F.G. Abath, F.L. Melo, R.P. Werkhauser, L. Montenegro, R. Montenegro, H.C. Schindler, Single-tube nested PCR using immobilized internal primers, Biotechniques 33 (2002).
[34] G. Frens, Controlled nucleation for the regulation of the particle size in monodisperse gold suspensions, Nat. Phys. Sci. 241 (1973) 20–22.
[35] N. Gan, H. Jin, T. Li, L. Zheng, Fe(3)O(4)/Au magnetic nanoparticle amplification strategies for ultrasensitive electrochemical immunoassay of alfa-fetoprotein, Int. J. Nanomed. 6 (2011) 3259–3269.
[36] M.D. Oliveira, C.A. Andrade, M.T. Correia, L.C. Coelho, P.R. Singh, X. Zeng, Impedimetric biosensor based on self-assembled hybrid cystein-gold nanoparticles and CramoLL lectin for bacterial lipopolysaccharide recognition, J. Colloid Interface Sci. 362 (2011) 194–201.
[37] D. Necas, P. Klapetek, C. Anderson, Gwyddion, 2008 http://www.gwyddion.net.
[38] H.Y. Park, M.J. Schadt, L. Wang, I.I.S. Lim, O.N. Njoki, S.H. Kim, M.Y. Jang, J. Luo, C.J. Zhong, Fabrication of magnetic Core@Shell Fe Oxide@Au nanoparticles for interfacial bioactivity and bio-separation, Langmuir 23 (2007) 9050–9056.
[39] I. Navratilova, P. Skladal, The immunosensors for measurement of 2 4-dichlorophenoxyacetic acid based on electrochemical impedance spectroscopy, Bioelectrochemistry 62 (2004) 11–18.
[40] A.J. Bard, L.R. Faulkner, Electrochemical Methods: Fundamentals and Applications, 2nd ed., Wiley, New York, 2000.
[41] J.G. Guan, Y.Q. Miao, Q.J. Zhang, Review impedimetric biosensors, J. Biosci. Bioeng. 97 (2004) 219–226.
[42] E. Katz, I. Willne, Probing biomolecular interactions at conductive and semiconductive surfaces by impedance spectroscopy: routes to impedimetric immunosensors, DNA-sensors, and enzyme biosensors, Electroanal 15 (2003) 913–947.
[43] H. Wang, H. Ohnuki, H. Endo, M. Izumi, Preparation of amperometric glucose biosensor based on 4-mercaptobenzoic acid, Phys. Procedia 14 (2011) 2–6.
[44] P. Geng, X. Zhang, W. Meng, Q. Wang, W. Zhang, L. Jin, Z. Feng, Z. Wu, Self-assembled monolayers-based immunosensor for detection of Escherichia coli using electrochemical impedance spectroscopy, Electrochim. Acta 53 (2008) 4663–4668.
[45] M.P. Costa, C.A. Andrade, R.A. Montenegro, F.L. Melo, M.D. Oliveira, Self-assembled monolayers of mercaptobenzoic acid and magnetite nanoparticles as an efficient support for development of tuberculosis genosensor, J. Colloid Interface Sci. 433 (2014) 141–148.
[46] M.D.L. Oliveira, M.L. Nogueira, M.T.S. Correia, L.C.B.B. Coelho, C.A.S. Andrade, Detection of dengue virus serotypes on the surface of gold electrode based on Cratylia mollis lectin affinity, Sens. Actuators B 155 (2011) 789–795.
[47] B.A. Boukamp, A package for impedance/admittance data analysis, Solid State Ionics 19 (1986) 136–140.
[48] F.B. Diniz, G.F. De Andrade, C.R. Martins, W.M. De Azevedo, A comparative study of epoxy and polyurethane based coatings containing polyaniline-DBSA pigments for corrosion protection on mild steel, Prog. Org. Coat. 76 (2013) 912–916.
[49] K. Kopecky, M. Giboda, E. Aldova, S.S. Dobahi, J. Radkovsky, Pilot studies on the occurrence of some infectious diseases in two different areas in south Yemen (Aden): part I. Parasitology, J. Hyg. Epidemiol. Microbiol. Immunol. 36 (1992) 253–261.
[50] D.S. Yole, K.T. Shamala, K. Kithome, M.M. Gicheru, Studies on the interaction of Schistosoma mansoni and Leishmania major in experimentally infected Balb/c mice, Afr. J. Health Sci. 14 (2007) 80–85.
[51] J. Nie, Y. Zhang, H. Wang, S. Wang, G. Shen, Superhydrophobic surface-based magnetic electrochemical immunoassay for detection of Schistosoma japonicum antibodies, Biosens. Bioelectron. 33 (2012) 23–28.
[52] M. Shohayeb, H. Arida, G.A.M. Mersal, M. El-Badawy, Development of a nanotechnology-based screen-printed biosensor for detection of schistosoma mansoni antibodies, Int. J. Electrochem. Sci. 11 (2016) 1337–1344.
[53] G.D. Liu, Z.Y. Wu, S.P. Wang, G.L. Shen, R.Q. Yu, Renewable amperometric immunosensor for Schistosoma japonium antibody assay, Anal. Chem. 73 (2001) 3219–3226.
[54] H.L. Che, S.P. Wang, Z.M. Wu, Z.Y. Wu, G.L. Shen, A new fluorescence immunoassay based on magnetic nanoparticles for Schistosoma japonicum antibodies, Chin. J. Anal. Chem. 36 (2008) 1455–1459.